



# Textile-reinforced mortar (TRM) versus fiber-reinforced polymers (FRP) in shear strengthening of concrete beams



Zoi C. Tetta, Lampros N. Koutas, Dionysios A. Bournas\*

Department of Civil Engineering, University of Nottingham, NG7 2RD, Nottingham, UK

## ARTICLE INFO

### Article history:

Received 15 December 2014

Received in revised form

3 March 2015

Accepted 16 March 2015

Available online 21 March 2015

### Keywords:

Fabrics/textiles

Carbon fibre

Debonding

Mechanical testing

Concrete strengthening

## ABSTRACT

This paper presents an experimental study on shear strengthening of rectangular reinforced concrete (RC) beams with advanced composite materials. Key parameters of this study include: (a) the strengthening system, namely textile-reinforced mortar (TRM) jacketing and fiber-reinforced polymer (FRP) jacketing, (b) the strengthening configuration, namely side-bonding, U-wrapping and full-wrapping, and (c) the number of the strengthening layers. In total, 14 RC beams were constructed and tested under bending loading. One of the beams did not receive any strengthening and served as control beam, eight received TRM jacketing, whereas the rest five received FRP jacketing. It is concluded that the TRM is generally less effective than FRP in increasing the shear capacity of concrete, however the effectiveness depends on both the strengthening configuration and the number of layers. U-wrapping strengthening configuration is much more effective than side-bonding in case of TRM jackets and the effectiveness of TRM jackets increases considerably with increasing the number of layers.

© 2015 The Authors. Published by Elsevier Ltd. This is an open access article under the CC BY license (<http://creativecommons.org/licenses/by/4.0/>).

## 1. Introduction and background

Structural retrofitting of existing reinforced concrete (RC) structures is a constantly growing need due to their deterioration (ageing, environmental induced degradation, lack of maintenance, and need for upgrading to meet the current design requirements). One of the most common structural deficiencies is the poor shear capacity of RC beams or bridge girders.

The use of fiber reinforced polymers (FRP) as externally bonded (EB) reinforcement in shear strengthening of RC members has become very popular over the last two decades. Following the studies of Triantafyllou 1998 [1] and Khalifa et al. [2] a big effort was made by researchers worldwide to further investigate or even improve this technique [i.e.3–9]; with all the results showing the high effectiveness of using EB FRP in shear strengthening of RC beams. However, the FRP strengthening technique has a few drawbacks mainly associated with the use of epoxy resins, namely high cost, poor performance in high temperatures, inability to apply on wet surfaces, as discussed in Ref. [10].

In an attempt to alleviate the problems arising from the use of epoxies, researchers have introduced a novel composite material,

namely textile-reinforced mortar (TRM), which combines advanced fibers in form of textiles (with open-mesh configuration) with inorganic matrices, such as cement-based mortars. Over the last decade it has been reported in the literature that TRM is a very promising alternative to the FRP retrofitting solution. TRM has been used for the strengthening of RC members [i.e.10–21] and, as well as for the seismic retrofitting of masonry-infilled RC frames [22]. Bousias et al. [23] applied TRM jackets for the seismic retrofitting of a large-scale RC 2-story building. Selected case studies of actual applications of TRM in the construction field can be found in ACI guidelines [24].

Shear strengthening of RC beams with TRM has been investigated by few researchers [25–29]. In these studies various parameters were investigated including the number of layers [25,27,29], the strengthening configuration [27] and the mechanical anchorage of the jackets [26,29]. A key parameter, namely the effectiveness of TRM versus FRP in shear strengthening of RC beams, has only been investigated on a limited number of specimens in Refs. [25] and [29]. In particular, in Ref. [25] it was concluded that TRM jackets are 45% less effective than their FRP counterparts, based on the results of two specimens retrofitted with closed jackets. Moreover, Tzoura and Triantafyllou [29] on the basis of four specimens retrofitted with U-jackets concluded that TRM jackets are nearly 50% less effective than their counterparts in case of non-anchored jackets, whereas in case of mechanically

\* Corresponding author. Tel.: +44 115 951 4096.

E-mail address: [Dionysios.Bournas@nottingham.ac.uk](mailto:Dionysios.Bournas@nottingham.ac.uk) (D.A. Bournas).

anchored jackets the TRM system is marginally inferior to the FRP system.

It is clear that the existing literature does not cover adequately the subject of comparing the two different strengthening systems (TRM versus FRP) when used in shear strengthening of concrete members. This paper presents the first systematic study on the effectiveness of TRM versus FRP jackets in shear strengthening of RC beams. The investigations address additional parameters including the number of layers and the strengthening configuration. Details are provided in the following sections.

## 2. Experimental programme

### 2.1. Test specimens and investigated parameters

The main objective of this study was to compare the effectiveness between TRM and FRP jacketing in shear strengthening of RC beams. A total of fourteen rectangular half-scale RC beams (cross-section dimensions of  $102 \times 203$  mm) were constructed and tested as simply supported in (non-symmetric) three-point bending as shown in Fig. 1a. The total length of the beams was equal to 1677 mm, whereas the effective flexural span was equal to 1077 mm (Fig. 1b), providing adequate anchorage length to the longitudinal reinforcement.

To emulate old detailing practices, the beams were designed to be deficient in shear in one of the two shear spans. To achieve this, the critical shorter shear span of 460 mm length did not include any transverse reinforcement, whereas the larger shear span included 8-mm diameter stirrups at a spacing of 75 mm (Fig. 2a). It should be noted that the effectiveness of FRP jackets is influenced by the presence and amount of stirrups [30]. However the aim of the present study was to directly assess the contribution of TRM and FRP jackets in the shear capacity of the strengthened beams excluding such an influence.

Strengthening was applied only at the critical shear span aiming to increase its shear resistance. By design, the shear force demand in order to develop the full flexural capacity of the (unretrofitted) beams was targeted to be 3 times their shear capacity. As shown in Fig. 2b two 16 mm-diameter and two 10 mm-diameter deformed bars were placed at the tension and compression zone of the rectangular beams, respectively. The geometrical ratio of tensile rebars was 2.2%.

The key investigated parameters of this study comprise: (a) the strengthening system (TRM or FRP), (b) the strengthening configuration, and (c) the number of layers. One beam was tested as-built without receiving strengthening and served as control specimen

(CON). The rest 13 beams were divided in two main groups (Fig. 3a). The first group comprised 8 beams strengthened with TRM jackets, whereas the second group comprised 5 beams strengthened with FRP jackets. Three different strengthening configurations were applied on each group's specimens, namely Side-Bonded jackets (SB), U-Wrapped jackets (UW) and Fully-Wrapped jackets (FW). For the SB and the UW configurations the specimens of the first group received from 1 to 3 TRM layers, whereas the specimens of the second group received 1 and 2 FRP layers. For the FW configuration the first group specimens received 1 and 2 TRM layers, while only one specimen of the second group received 1 FRP layer. The notation of specimens is X<sub>Y</sub>N, where X refers to the strengthening configuration (SB, UW and FW), Y denotes the type of the binding material (M for Mortar or R for Resin) and N denotes the number of layers (1, 2 or 3).

### 2.2. Materials and strengthening procedure

The specimens were cast in groups of four using the same concrete mix design. The compressive strength and the tensile splitting strength of the concrete were experimentally obtained on the day of testing by conducting standard tests on cylinders of 150 mm-diameter and of 300 mm - height. The results are summarized in Table 1 (average values of 3 specimens). The 16 and 10 mm-diameter longitudinal bars had a yield stress of 547 MPa and 552 MPa, respectively (average of 3 specimens), while the standard deviation is 6.24 MPa and 2.66 MPa, respectively. The corresponding values for the 8 mm-diameter bars used for stirrups were 568 MPa and 2.71 MPa, respectively.

The same reinforcement was used in both strengthening systems; the only difference between the two systems was the binding material (epoxy resin in case of FRP and cementitious mortar in case of TRM). This reinforcement comprised a textile with equal quantity of high-strength carbon fibers in two orthogonal directions (Fig. 3b). The weight of the textile was  $348 \text{ g/m}^2$ , whereas its nominal thickness (based on the equivalent smeared distribution of fibers) was 0.095 mm. According to the manufacturer datasheets the tensile strength and the modulus of elasticity of the carbon fibers were 3800 MPa and 225 GPa, respectively.

For the specimens receiving mortar as binding material an inorganic dry binder was used, consisting of cement and polymers at a ratio of 8:1 by weight. The water-binder ratio in the mortar was 0.23:1 by weight, resulting in plastic consistency and good workability. Table 2 summarizes the strength properties of the mortar (average values of 3 specimens) obtained experimentally on the day of testing using prisms of  $40 \times 40 \times 160$  mm dimensions,

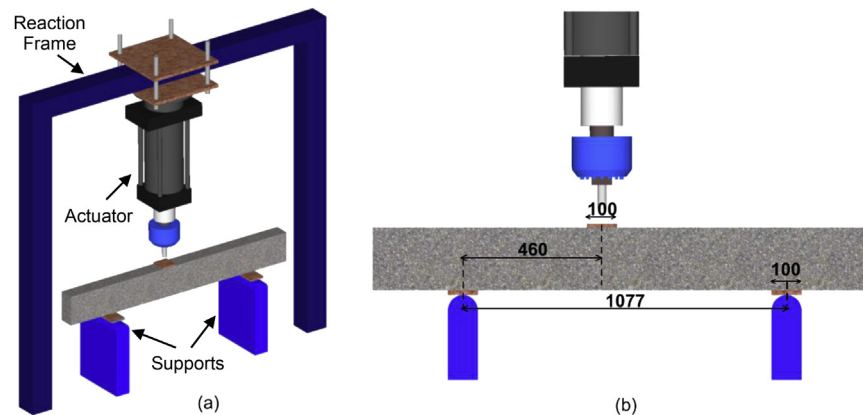


Fig. 1. Test set-up: (a) Overall 3D view; (b) front view.

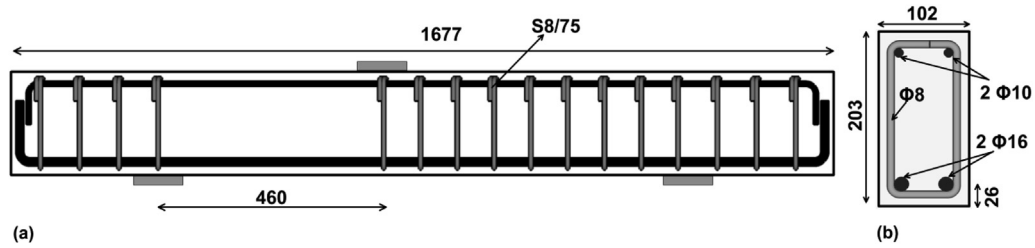


Fig. 2. (a) Beam geometry and reinforcement; (b) cross section (dimensions in mm).

	Textile + Cement based mortar	Textile + Epoxy resin
	TRM	FRP
SB	SB_M1 SB_M2 SB_M3	SB_R1 SB_R2
UW	UW_M1 UW_M2 UW_M3	UW_R1 UW_R2
FW	FW_M1 FW_M2	FW_R1

Fig. 3. (a) Groups of specimens; (b) geometry of the carbon textile used in this study (dimensions in mm).

**Table 1**  
Concrete strength on the day of testing.

Group of specimens	Compressive strength (MPa)	Standard deviation (MPa)	Tensile splitting strength (MPa)	Standard deviation (MPa)
CON; SB_R1; FW_R1; FW_M2	21.6	0.60	2.36	0.22
SB_R2; SB_M1; FW_M1	21.6	0.66	2.66	0.16
UW_R1; UW_R2; UW_M1; UW_M2	23.8	0.50	2.73	0.11
SB_M2; SB_M3; UW_M3	22.6	0.53	2.81	0.14

according to the EN 1015-11 [31]. For the specimens receiving epoxy adhesive as binding material, a commercial adhesive (two-part epoxy resin with a mixing ratio 4:1 by weight, Sikadur<sup>®</sup>–330) was used with an elastic modulus of 3.8 GPa and a tensile strength of 30 MPa (according to the manufacturer datasheets). The glass transition temperature ( $T_g$ ) of the epoxy resin is equal to 68 °C. The low viscosity of the adhesive allowed for the impregnation of the textile meshes by using a plastic roll.

Prior to strengthening a thin layer of concrete cover was removed and a grid of grooves (2–3 mm deep) was created as shown

in Fig. 4a, using a grinding machine. The corners of the specimens receiving UW or FW jackets were rounded to a radius of approximately 15 mm in order to avoid stresses concentration. For FRP-jacketed specimens the first textile layer was applied on the top of the first resin layer and was then impregnated in-situ with resin using a plastic roll (Fig. 4b). Special care was taken to ensure the full impregnation of the textile fibers with resin. If more than one textile layers were to be applied, the process was repeated until the application of all the layers was completed. For TRM-jacketed specimens the mortar was applied in approximately 2 mm-thick

**Table 2**  
Mortar strength on the day of testing.

Group of specimens	Flexural strength (MPa)	Standard deviation (MPa)	Compressive strength (MPa)	Standard deviation (MPa)
SB_M1; UW_M1; FW_M1; UW_M2	10.30	1.03	31.1	1.10
SB_M2; FW_M2	9.21	0.82	28.2	1.34
SB_M3; UW_M3	8.64	0.52	26.9	1.11

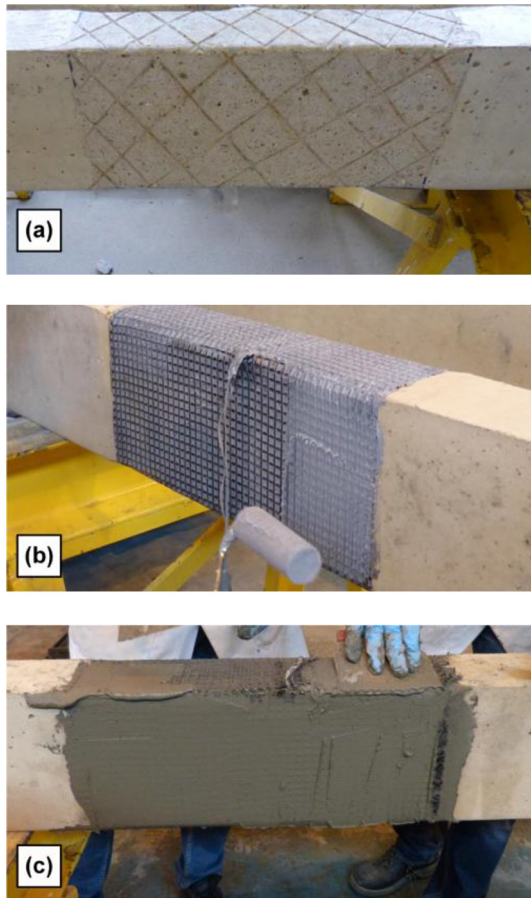


**Fig. 4.** (a) Prepared concrete surface before strengthening; (b) impregnation of the textile fibers with epoxy resin; (c) application of an extra layer of mortar on the top of the final textile layer.

layers with a smooth metal trowel. After application of the first mortar layer on the (dampened) concrete surface, the textile was applied and pressed slightly into the mortar, which protruded through all the perforations between the fiber rovings. The next mortar layer covered the textile completely, and the operation was repeated until all textile layers were applied and covered by mortar (Fig. 4c). Of crucial importance in this method, as in the case of epoxy resins, was the application of each mortar layer while the previous one was still in a fresh state.

### 2.3. Experimental setup and procedure

The beams were subjected to monotonic loading using a stiff steel reaction frame and a three-point bending set-up configuration as shown in Fig. 1a. A vertically positioned servo-hydraulic actuator was used for the application of the load at a displacement rate of 0.02 mm/s. As illustrated in Fig. 5a the vertical displacement was measured at the position of load application using external Linear Variable Differential Transducer (LVDT); the displacement measured from this sensor was used to plot the load–displacement curve for each specimen. Moreover, measurements from the potentiometers placed at the critical shear span in one side of the beam, were utilized to monitor the average shear strain of the span (Fig. 5b).

Additionally, the Digital Image Correlation (DIC) technique was employed to monitor relative displacements within the critical

shear span, using two high-resolution cameras (on the side of the beam which was free of sensors). Finally, strain gauges were mounted to the longitudinal bars at the cross-section of maximum moment to monitor possible yielding of the steel reinforcement. It is noted that all data was synchronized and recorded using a fully-computerized data acquisition system.

### 3. Experimental results

The response of all specimens tested is given in Fig. 6 in the form of load–displacement curves. Key results are also presented in Table 3. They include: (1) The peak load. (2) The observed failure mode. (3) The shear resistance of the critical shear span,  $V_R$ , which is the shear force in the critical span at peak load. (4) The contribution of the jacket to the total shear resistance,  $V_f$ , which is calculated as the shear resistance of the strengthened specimen minus the shear resistance of the control specimen. (5) The shear strengthening effectiveness which is expressed by the ratio of the shear resistance of a strengthened specimen,  $V_{R, str}$ , to the shear resistance of the control beam,  $V_{R, con}$ . (6) The average shear strain of the critical shear span at peak load,  $\gamma_{Pmax}$ . (7) The shear deformation capacity enhancement of the critical span as expressed by the ratio of the  $\gamma_{Pmax, str}$  of the strengthened specimen to the  $\gamma_{Pmax, con}$  of the control beam.

The average shear strain at the critical shear span,  $\gamma$ , was obtained from readings of the two potentiometers placed in X configuration (Fig. 5b) according to Eq. (1).

$$\gamma = \frac{(d'_1 - d)d - (d'_2 - d)d}{2Lh} \quad (1)$$

The control beam (CON) failed in shear at an ultimate load of 51.8 kN after the formation of a large shear crack in the critical span as shown in Fig. 7. The strong dowel action provided by the longitudinal reinforcement prevented the sudden drop of load and contributed to the residual shear resistance of the beam after the peak load.

All beams strengthened with SB or UW FRP jackets failed in shear at an ultimate load substantially higher than that of the control beam; thus confirming the effectiveness of FRP jacketing in shear strengthening of RC members. The peak load attained by specimens SB\_R1, UW\_R1, SB\_R2 and UW\_R2 was 105, 113.4, 124.5 and 126.2 kN, respectively, which yields 103%, 119%, 140% and 143% increase in the shear capacity, respectively. In all these specimens failure occurred due to FRP debonding; the excellent bond between the resin and the concrete substrate resulted in peeling off of the FRP jackets with part of the concrete. It was observed that in specimens with SB jackets the part of concrete that peeled off was thinner with respect to the specimens with UW jackets (Fig. 8a and Fig. 8b). Debonding of FRP reinforcement was initiated from the point of load application and propagated instantly to the support (Fig. 8c). One layer of FW FRP jacket resulted in enhancing at least 2.8 times the shear capacity. Specimen FW\_R1 reached its ultimate moment capacity at a load of 150.3 kN and failed due to concrete crushing after yielding of the tensile longitudinal reinforcement (at approximately 140 kN – Fig. 8d). This confirmed the high effectiveness of closed FRP jackets. However, the use of closed jackets is not feasible in beams of typical RC buildings or bridge girders due to the presence of concrete slabs or decks, respectively.

With only the exception of specimen FW\_M2 which failed in flexure, all the TRM-strengthened specimens failed in shear and displayed considerably higher shear resistance (from approximately 10% up to approximately 150%) compared to the control specimen. The behaviour of TRM-strengthened specimens is

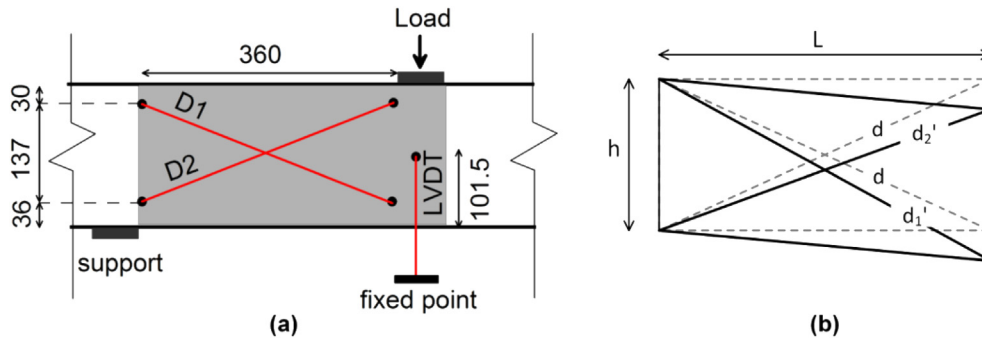


Fig. 5. (a) Configuration of the two potentiometers (D1, D2) and the LVDT at the shear-critical span; (b) shear deformation measurement by X configuration.

described below into groups depending on the number of strengthening layers.

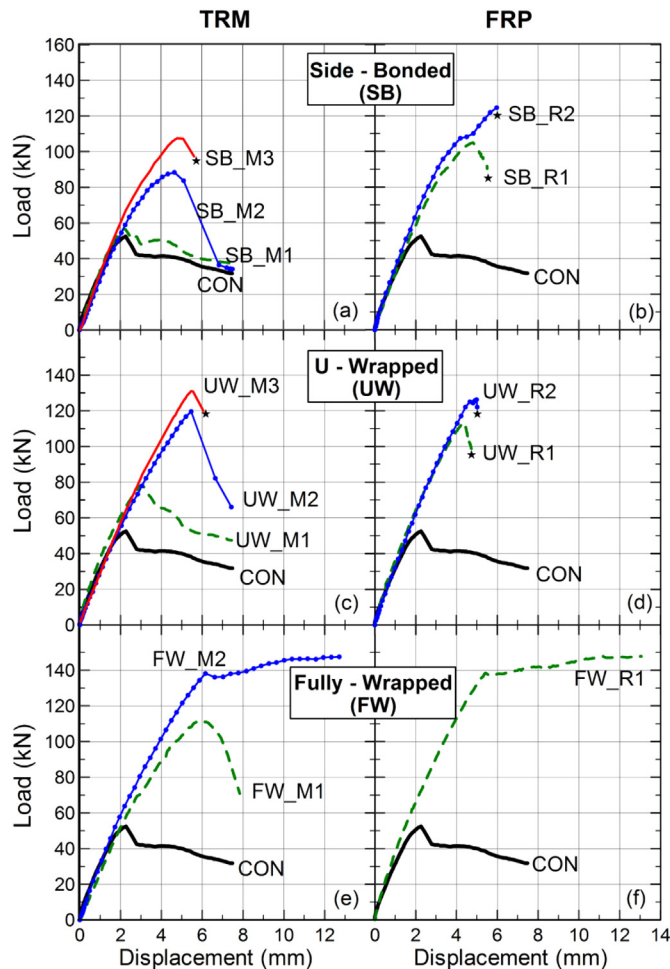
Specimens SB\_M1, UW\_M1 and FW\_M1, which received one TRM layer, reached an ultimate load of 56.6, 78.2 and 111.2 kN, respectively. The corresponding increase in their shear capacity was equal to 9%, 51% and 115%. The failure of these specimens was associated with damage of the TRM jackets (Fig. 9a–c). The load-drop in these specimens was attributed to the following local phenomena: (a) slippage of the vertical fiber rovings through the mortar and (b) partial rupture of the fibers crossing the shear crack. Going from the SB to the UW and finally to the FW configuration,

the second phenomenon is more pronounced, whereas the first one tends to be eliminated. The nature of these local phenomena did not allow for a brittle failure mode. In fact, after the peak load was reached, relatively soft load degradation was recorded. As can be seen in Fig. 6(a,c,e) for specimens strengthened with one layer the descending branch is quite smooth for SB jackets and becomes less smooth in UW and FW jackets, respectively.

Specimens SB\_M2 and UW\_M2 failed in shear at a load of 88.7 and 120.2 kN, respectively. Compared to the control specimen the increase in the shear resistance was equal to 71% and 132%, respectively. Failure in these specimens was attributed to debonding of the TRM jacket at a large part (approximately 2/3) of the shear span which was accompanied by peeling off of the concrete cover (Fig. 9d and e). This type of failure, although it was brittle, it was not as explosive as in the case of FRP-strengthened beams. Finally specimen FW\_M2, after the formation of a shear crack at 70 kN, reached its ultimate moment capacity and (identically to FW\_R1) failed in flexure due to concrete crushing at the compression zone (Fig. 9f).

Specimens SB\_M3 and UW\_M3 failed in shear at even higher loads (108.9 and 131.1 kN, respectively) when compared to the corresponding specimens strengthened with two TRM layers (SB\_M2 and UW\_M2). The shear resistance of specimens SB\_M3 and UW\_M3 was increased by 110% and 153%, respectively, with respect to the control specimen. Specimen SB\_M3 (Fig. 9g) failed in a similar way with specimen SB\_M2 (Fig. 9d), whereas the failure mode of specimen UW\_M3 was unique among all TRM-strengthened specimens. In the latter case debonding of the U-jacket occurred at the full-length of the shear span (Fig. 9h) and was as explosive as in case of all FRP-strengthened specimens.

Fig. 10 presents the load versus average shear strain curves for all specimens which are plotted up to peak load (specimens FW\_M2 and FW\_R1 that failed in flexure are plotted up to yielding). The values of shear strain at peak load ( $\gamma_{pmax}$ ) are presented in Table 3. Strengthening the beams with TRM or FRP jackets resulted in an increase in the average shear strain over the critical shear span, which at peak load varied from 1.32 to 3.38 times (compared to the control specimen). This increase is mainly attributed to redistribution of shear stresses in the shear span, which ultimately led to a more dense crack pattern and hence to an increased shear deformation capacity. It is also concluded that, in general, higher average strains were developed in TRM-retrofitted specimens compared to their FRP counterparts.



\* sudden failure of beam

Fig. 6. Load versus vertical displacement curves for all tested specimens.

## 4. Discussion

### 4.1. Strengthening configuration and number of layers

The curves in Fig. 11a illustrate the effect of the strengthening configuration (SB, UW or FW) on the shear capacity enhancement

**Table 3**  
Summary of test results.

Specimen	(1) Peak load (kN)	(2) Failure mode	(3) $V_R$ (kN)	(4) $V_f$ (kN)	(5) Shear strengthening effectiveness $V_{R,STR}/V_{R,CON}$	(6) Shear strain at peak load (%), $\gamma_{Pmax}$	(7) Shear deformation capacity enhancement $\gamma_{Pmax,STR}/\gamma_{Pmax,CON}$
CON	51.8	shear <sup>a</sup>	29.7	–	–	1.51	–
SB_M1	56.6	shear <sup>b</sup>	32.4	2.7	1.09	2.00	1.32
UW_M1	78.2	shear <sup>b</sup>	44.8	15.1	1.51	4.00	2.65
FW_M1	111.2	shear <sup>b</sup>	63.7	34.0	2.15	3.78	2.50
SB_M2	88.7	shear <sup>c</sup>	50.8	21.1	1.71	3.63	2.40
UW_M2	120.2	shear <sup>c</sup>	68.8	39.2	2.32	4.34	2.87
FW_M2	152.8	flexural	87.5	57.8 <sup>d</sup>	2.95	–	–
SB_M3	108.9	shear <sup>c</sup>	62.4	32.7	2.10	5.10	3.38
UW_M3	131.1	shear <sup>c</sup>	75.1	45.4	2.53	3.07	2.03
SB_R1	105.0	shear <sup>c</sup>	60.2	30.5	2.03	4.82	3.19
UW_R1	113.4	shear <sup>c</sup>	64.9	35.3	2.19	3.33	2.21
FW_R1	150.3	flexural	86.1	56.4 <sup>d</sup>	2.90	–	–
SB_R2	124.5	shear <sup>c</sup>	71.3	41.6	2.40	3.26	2.16
UW_R2	126.2	shear <sup>c</sup>	72.3	42.6	2.43	2.54	1.68

<sup>a</sup> Tensile diagonal cracking.

<sup>b</sup> Slippage of the vertical fiber rovings through the mortar and partial fibers rupture.

<sup>c</sup> Debonding of the jacket.

<sup>d</sup> This value can be considered as a lower limit of  $V_f$  due to the flexural failure.

( $V_f/V_{con} \times 100\%$ ). In FRP-strengthened specimens, the shear capacity was only marginally increased when UW jackets were applied instead of SB ones. On the other hand in TRM-strengthened specimens, the effectiveness of the UW jackets (expressed as the shear capacity enhancement) was 5.5 and 1.85 times the effectiveness of the SB jackets for 1 and 2 layers, respectively. Therefore, the benefit of applying UW instead of SB jackets was more pronounced in TRM than FRP system, especially as the number of layers increased. Finally, FW jacketing was the most effective configuration for both strengthening systems. In particular, the effectiveness of the FW jacket was 2.2 times the UW jacket effectiveness in case of one TRM layer, and at least 1.5 times in case of two TRM layers. For one FRP layer FW jacket was at least 1.6 times more effective than the UW jacket.

The effect of the number of layers on the shear capacity enhancement for SB and UW strengthening configurations is illustrated in Fig. 11b. Doubling the amount of reinforcement (two layers instead of one) resulted in dramatic increase of the TRM jackets effectiveness. In particular, this increase was equal to 7.8 and 2.6 times for the SB and UW jackets, respectively. The corresponding increase when resin was used as binder was 1.35 and 1.2 times. The latter is consistent with the typical behaviour in FRP jackets in which increasing the amount of EB reinforcement results in limiting the effectiveness of FRP strengthening. To further investigate this effect on TRM jackets, beams with three layers were also tested for both SB and UW strengthening configurations. As



**Fig. 7.** Dominant shear crack in the control beam.

shown in Fig. 11b, applying a third TRM layer resulted in strength increase of 1.55 and 1.15 times for SB and UW jackets, respectively. In the case of UW TRM jackets, increasing the number of layers from two to three had approximately the same effect as in FRP jackets for the increase from one to two layers. This trend is clearly illustrated Fig. 11b from the slope of  $V_f/V_{con}$  – no. of layers curves.

A possible explanation for the difference between the two strengthening systems, regarding the effect of increasing the number of layers from one to two, could be found in the observed failure modes. As described in Section 3, all specimens retrofitted with FRP jackets exhibited the same failure mode which is associated to the failure of the concrete substrate with no damage in the composite jackets. However, in the case of TRM-retrofitted specimens a change in the failure mode was witnessed when the number of layers was increased from one to two or three. In specific, when one layer was applied the failure was attributed to local damage of the TRM jacket; the vertical fiber rovings crossing the developed shear crack at the jacket experienced a combination of partial rupture and slippage through the mortar (Fig. 9a and b). The increase in the number of layers in that case prevented these local phenomena and as a result the damage was shifted to the concrete substrate.

When preventing the local damage of the TRM jacket, due to partial rupture and slippage through the mortar (Fig. 9a and b), one of the following failure modes will occur: (a) debonding at the interface between the jacket and the concrete substrate, (b) inter-laminar shear failure at the interface between two textile layers, or (c) peeling off of the concrete substrate. The first two, which are premature failure modes, are more likely to happen for low values of mortar tensile strength which could lead to its bond failure. The benefit of using a relatively high-strength mortar (like the one used in this study) is that excellent bond conditions can be achieved, resulting in the development of the third failure mode and therefore yielding the best results in terms of shear capacity enhancement.

The arising question at this point is why the relatively poor behaviour of the TRM jacket at the local level was significantly improved when a second layer of textile was provided. The authors believe that the key answer to this question could be found in the mechanism of transferring forces from the textile reinforcement to the matrix. It seems that by providing just a second layer of textile, the mechanical interlock, which is the main mechanism of

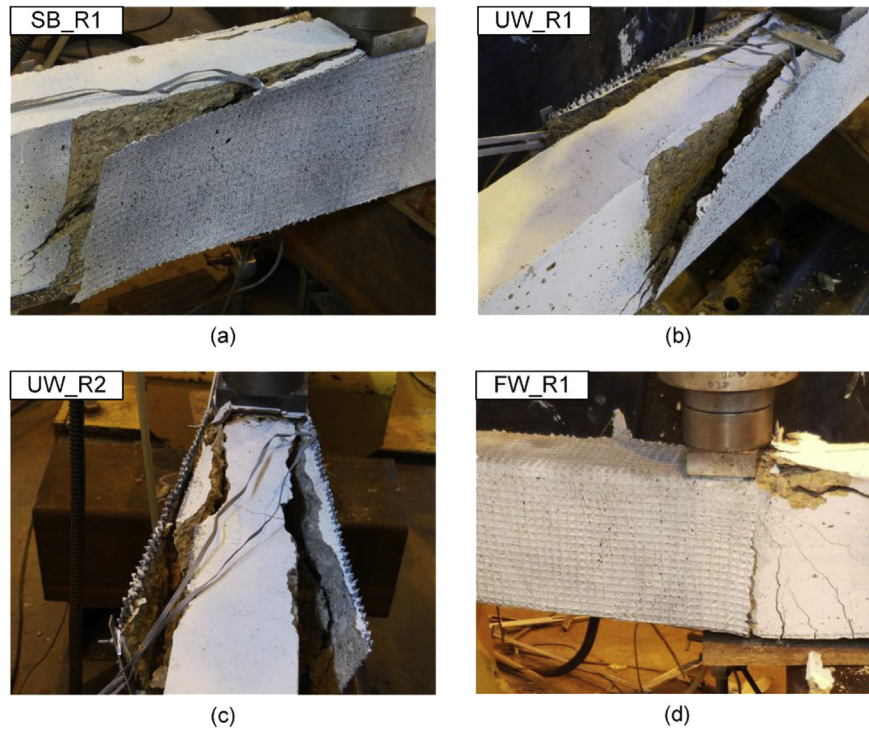


**Fig. 8.** (a) FRP debonding in SB strengthening configuration; (b), (c) FRP debonding in UW strengthening configuration; (d) flexural failure of specimen with FW FRP jacket.

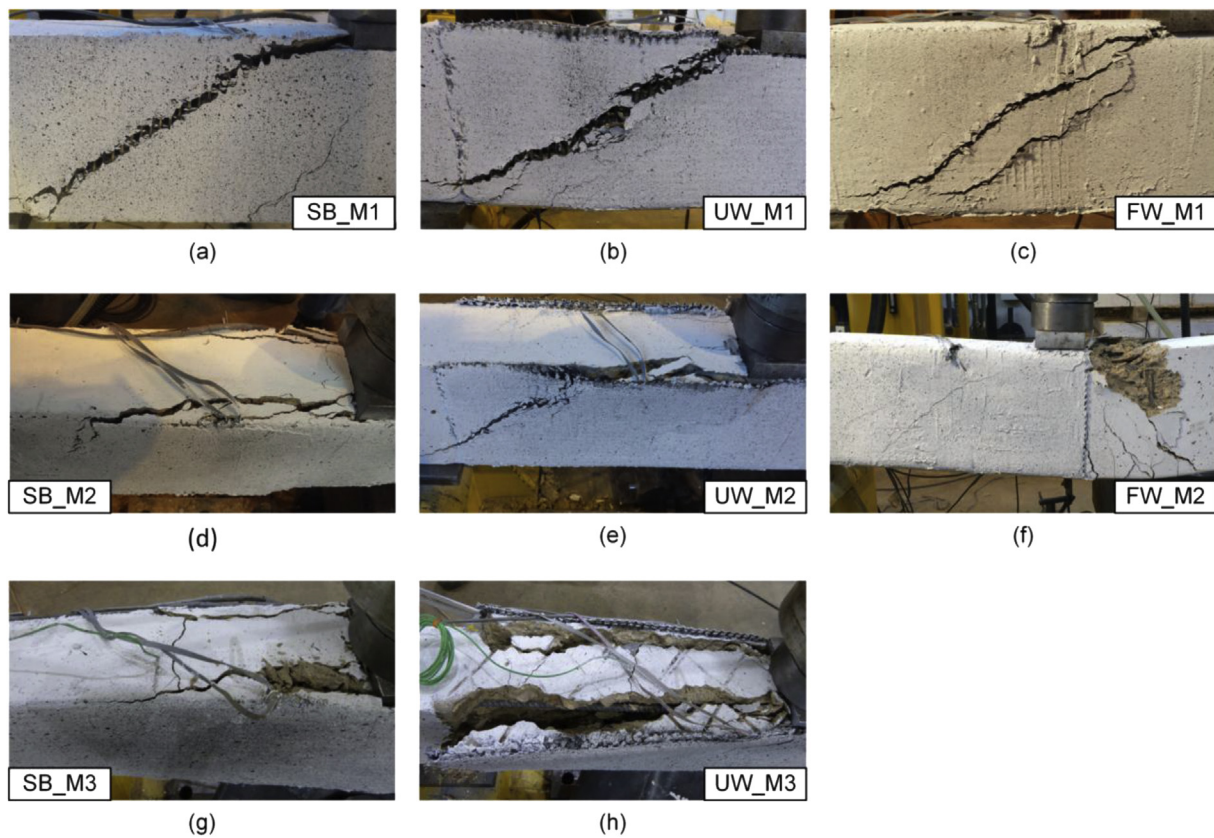


**Fig. 9.** Failure modes of TRM-retrofitted specimens: (a)–(c) Specimens SB\_M1, UW\_M1 and FW\_M1 – local damage of the jacket; (d), (e) SB\_M2 and UW\_M2 – debonding of the jacket over a large area of the shear span: peeling off of the concrete cover; (f) FW\_M2 – flexural failure despite the shear cracking of the TRM jacket; (g) SB\_M3 – debonding of the jacket over a large area of the shear span: peeling off of the concrete cover; and (h) UW\_M3 – abrupt debonding of the TRM jacket over the whole area of the shear span: peeling off of the concrete cover.

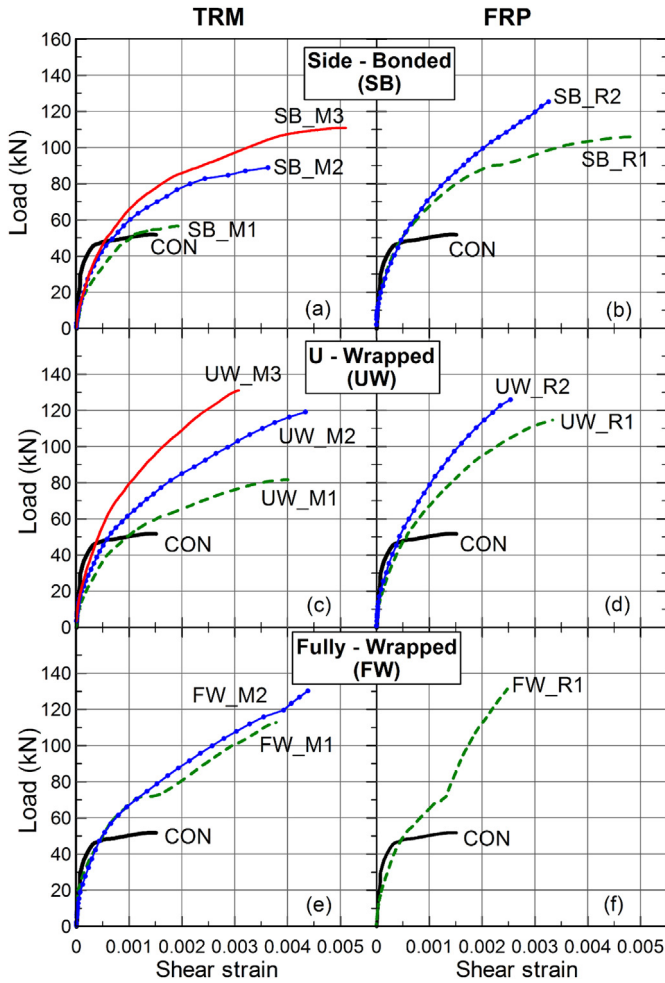


Fig. 10. Load versus average shear strain curves.

transferring forces from the reinforcement to the matrix in TRM systems, is drastically improved. This improvement might be attributed to the fact that two (at least) overlapping textile layers create a denser mesh-pattern than one. This happens due to the possible offset between the two layers (Fig. 12). Provided that mortar will not fail in shear; the denser mesh-pattern in turn

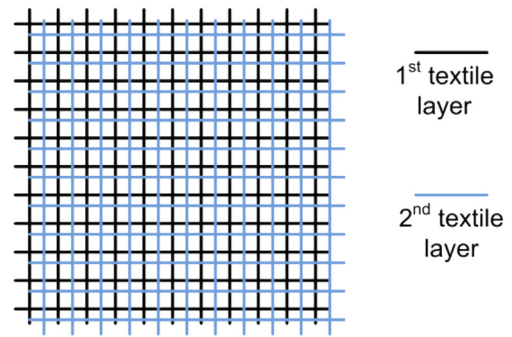


Fig. 12. Overlapping of two textiles with an offset.

creates conditions for improved mechanical interlocking characteristics, which ultimately results in altering the failure mode.

#### 4.2. Deformation aspects of jackets based on DIC

The response of the TRM and FRP SB and UW jackets, as a means of vertical deformations distribution along the beam height, was captured using the DIC method and is presented in Fig. 13. Each curve illustrates the relative displacement of each point along the beam height with respect to the bottom of the beam (at the middle cross-section of the critical shear span) at the instant of peak load. For the sake of comparison, the corresponding curve of the control beam is also plotted in all curves.

As illustrated in Fig. 13 the control beam exhibited concentration of the vertical deformations at a specific level, which is related to the development of a single shear crack at that level (at around 130–140 mm from the bottom of the beam). The specimens with one TRM layer exhibited identical behaviour, with concentration of the deformations at a single level. Better distribution of deformations was observed in the rest specimens, indicating that the jackets were activated over a broader area due to better redistribution of stresses. Fig. 13 provides the evidence that in TRM jackets the force transferring mechanism is being modified with additional layers, thus resulting in a performance of the TRM jackets similar to the performance of the FRP jackets. However, the distribution of deformations in FRP jackets is consistently better than the TRM jackets for the same number of layers.

Another interesting aspect of the behaviour of the TRM jackets is associated to their strengthening configuration. SB jackets deform

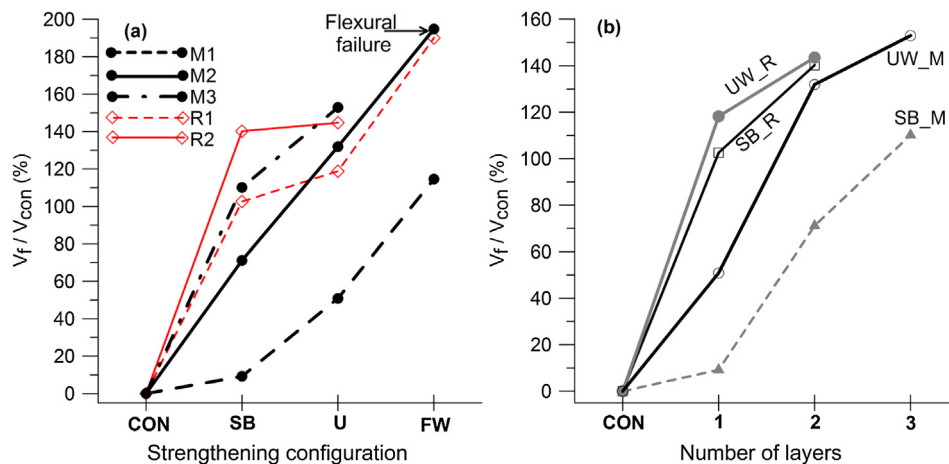


Fig. 11. (a) Effect of strengthening configuration on the shear capacity enhancement; (b) effect of number of layers on the shear capacity enhancement.

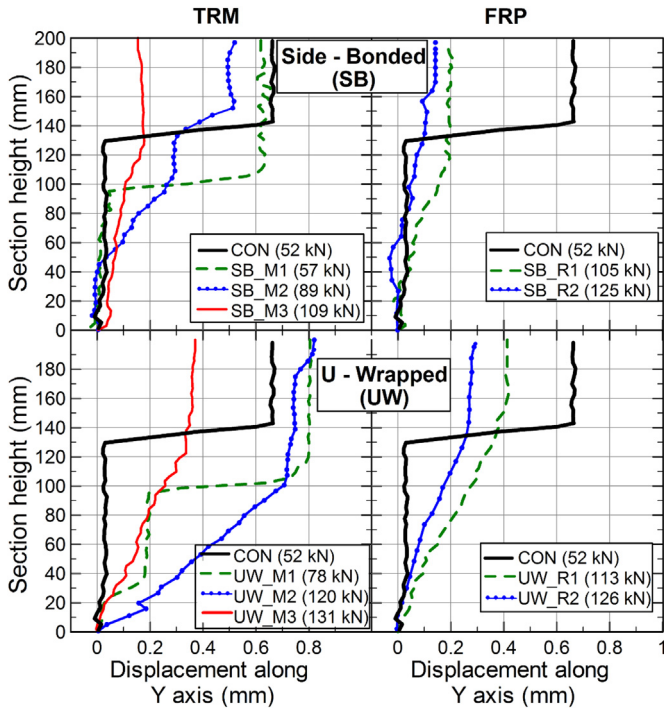


Fig. 13. Relative vertical displacements along the beam height at the central cross-section of the critical shear span, at the instant of peak load.

at the central region along the beam height (with the two ends being almost inactive), whereas UW jackets deform from the bottom level to a level in the central region, thanks to the anchorage of the jackets at the bottom corner of the beams. Photos of the vertical deformations field of the TRM jackets, obtained through DIC at peak load are shown in Fig. 14. From there it is also evident that in TRM jackets with two or three layers the vertical deformations are distributed over a broader region of the shear span, when compared to TRM jackets with one layer.

### 5. Effective stress and TRM versus FRP effectiveness factor: design aspects

For calculating the FRP contribution to the shear capacity of RC members most of the design models use the effective stress of the

FRP ( $\sigma_{eff}$ ), which can ideally be described as the average stress of the fibers crossing the shear crack. Given the effective stress, the shear force carried by the FRP,  $V_f$ , can be calculated using the Eq. (2) [1] under the assumptions that: (a) the shear crack forms an angle  $\theta = 45^\circ$  with respect to the member axis, and (b) fibers crossing the crack are perpendicular to the member axis.

$$V_f = \rho_f \sigma_{eff} b_w 0.9d \quad (2)$$

Where  $\rho_f$  is the geometrical reinforcement ratio of the composite material, expressed as  $\rho_f = 2t_f/b_w$  (this is valid for continuous FRP sheets and not for FRP strips),  $b_w$  is the width of the beam,  $d$  is the effective depth of the member section, and  $t_f$  is the total thickness of the composite material (usually taken equal to the thickness of the fabric times the number of layers).

According to Triantafillou and Papanicolaou [25] the format of Eq. (2) can also be used for the calculation of the shear force carried by TRM jackets. In particular, assuming that: (a) the shear crack forms an angle  $\theta = 45^\circ$  with respect to the member axis, and (b) a two-directional textile is applied with the one direction of fibers being perpendicular to the member axis and the other being parallel to the member axis, then Eq. (2) can be used without any modifications.

Application of Eq. (2) to the (SB and UW jacketed) beams tested in this study with  $t_f$  equal to the nominal thickness of the fibers, results in the values of  $\sigma_{eff}$  and  $\varepsilon_{eff}$  given in Table 4 ( $\varepsilon_{eff}$  is the so-called effective strain and is calculated by dividing  $\sigma_{eff}$  by the modulus of elasticity of the fibers,  $E_f$ ). In addition, Table 4 includes the effectiveness factor  $k$ , which is defined as the ratio of the TRM to FRP jackets effective stress. It should be noted that Triantafillou and Papanicolaou [25] obtained a value of  $k = 0.55$  from tests on two rectangular RC beams retrofitted with TRM and FRP closed jackets. In the present study the effectiveness factor  $k$  varies significantly not only for different strengthening configuration (SB or UW jacketing), but also for different number of layers. In particular, it varies from 0.09, which corresponds to one layer of SB jacket, to 0.92 which corresponds to two layers of UW jacket. Hence, the results of this study indicate that TRM jackets are less effective than FRP jackets as in Ref. [24], but the effectiveness is sensitive to parameters such as the strengthening configuration and the number of layers. By increasing the number of layers from one to two the effectiveness factor increases substantially, whereas the same happens when UW jackets are applied instead of SB jackets.

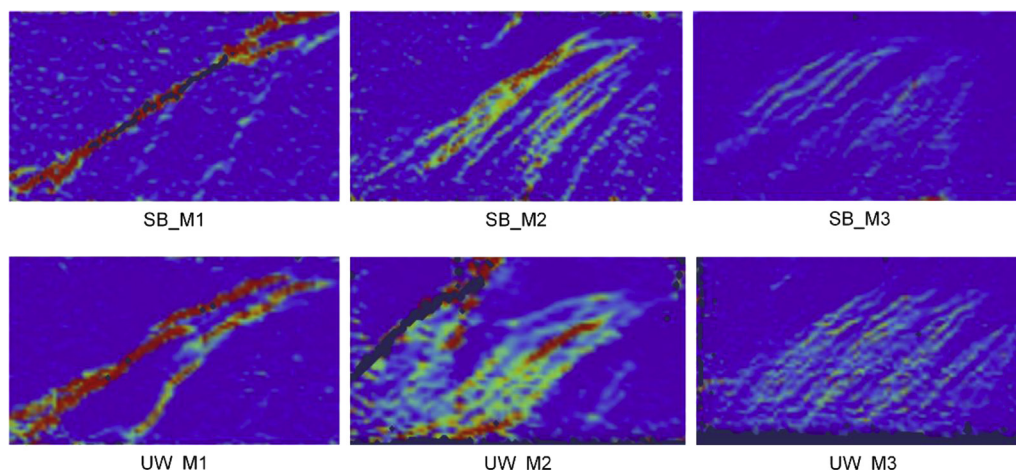


Fig. 14. Field of vertical axis deformations in the critical shear span of TRM-retrofitted specimens at the instant of peak load.

**Table 4**  
Experimental values of effective strains and effectiveness factor for SB and UW jackets.

	Side-bonded jackets				U-wrapped jackets			
	1 layer		2 layers		1 layer		2 layers	
	TRM (SB_M1)	FRP (SB_R1)	TRM (SB_M2)	FRP (SB_R2)	TRM (UW_M1)	FRP (UW_R1)	TRM (UW_M2)	FRP (UW_R2)
Effective stress, $\sigma_{eff}$ (MPa)	90	990	344	675	491	1168	637	693
Effective strain, $\epsilon_{eff}$ (‰)	0.40	4.40	1.53	3.00	2.18	5.19	2.83	3.08
TRM versus FRP effectiveness factor, $k$ ( $\sigma_{eff,TRM}/\sigma_{eff,FRP}$ )	0.09		0.51		0.42		0.92	

Fig. 15 plots the experimentally obtained effective strains versus  $\rho_f E_f/f_c^{2/3}$  curves, for different strengthening systems (TRM versus FRP) and configurations (SB versus UW), together with the curve corresponding to the formula suggested in Ref. [32] for calculating  $\epsilon_{eff}$  in FRP jackets. The trend of the experimental values for FRP jackets is descending for increasing values of  $\rho_f E_f/f_c^{2/3}$  which is in agreement with the theoretical curve. On the contrary, TRM jackets do not follow the same trend; there is significant increase of  $\epsilon_{eff}$  for low  $\rho_f$  values, whereas for higher  $\rho_f$  values this effect is eliminated. This is explained by the fact that TRM jackets do not experience a full-composite action for low values of  $\rho_f$ .

It seems that after a critical value of  $\rho_{f,crit}$ , TRM jackets develop full-composite action and behave similar to FRP jackets (e.g. specimen UW\_M3). It should be noted that the development of full-composite action of TRM jackets depends on several factors such as the mortar mechanical properties, the strengthening configuration, the number of layers and possibly the textile geometry. Further investigation regarding this critical value is beyond the scope of this paper. Future studies should be directed towards investigating the effectiveness between TRM and FRP jackets for a wider range of  $\rho_f$  values in parallel with the validation of the complex local phenomena in TRM jackets that strongly influence their effectiveness.

**6. Conclusions**

This paper presents an experimental investigation on the effectiveness of TRM and FRP jackets in shear strengthening of rectangular RC beams. Key parameters of this study were: (a) the

strengthening system (TRM versus FRP), (b) the strengthening configuration (SB, UW or FW jacketing) and (c) the number of layers. For this purpose, fourteen shear-deficient beams were subjected to three-point bending under monotonic loading: one was tested as-built, whereas the rest thirteen were strengthened prior to testing. The main conclusions drawn from this study are summarized as follows:

- TRM is generally less effective in increasing the shear capacity of RC beams than FRP jacketing, but the effectiveness depends on both the strengthening configuration and the number of layers. The TRM versus FRP effectiveness factor varies from 0.09, which correspond to one layer of side-bonded jacket, to 0.92, which correspond to two layers of U-wrapped jacket.
- TRM jackets are more effective in increasing the beams deformation capacity (expressed as the average shear strain of the shear-critical span) than FRP jackets.
- U-wrapping (UW) strengthening configuration is much more effective than side-bonding (SB) in case of TRM jackets. On the contrary, in case of FRP jackets the UW configuration was found only slightly more effective than the SB configuration. Full-wrapping (FW) is the most effective strengthening configuration for both strengthening systems.
- A major difference between TRM and FRP strengthening systems is observed by increasing the number of layers from 1 to 2. In particular, the effectiveness of FRP jackets increases by 1.35 and 1.2 times for SB and UW configurations, respectively, whereas the effectiveness of TRM jackets increases by 7.8 and 2.6 times, respectively.
- The considerably higher effectiveness of TRM jackets when two instead of one textile layers are applied is linked to the change in the failure mode. The local damage the TRM jackets experience when one layer is applied (partial fibers rupture and slippage of fiber filaments through the mortar), is being shifted to the concrete substrate when two layers are applied (debonding of the jacket with peeling-off of the concrete). This is attributed to the better mechanical interlock conditions created by the overlapping of at least two textile layers.

The above conclusions should be treated carefully as they are based on limited number of half-scale specimens. In this respect, future research should be directed towards investigating a wide range of jackets reinforcing ratio for different strengthening configurations, as well as testing of full-scale beams retrofitted with TRM jackets in order to increase the level of confidence, especially on the effective strain, and thus to allow for the development of reliable design models.

**Acknowledgements**

The authors wish to thank MSc students Brwa Salihi and Mouza Al Salim, the lab managers Tom Buss and Mike Langford, the chief

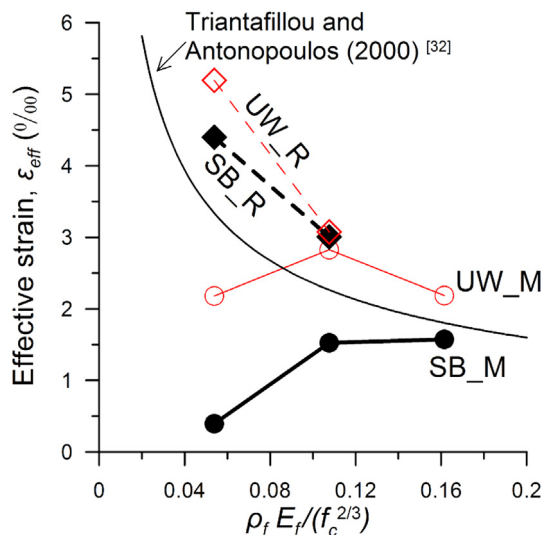


Fig. 15. Experimentally obtained effective strains versus  $\rho_f E_f/f_c^{2/3}$  and comparison with the theoretical curve of Triantafyllou and Antonopoulos (2000) model.

technician Nigel Rook, and the technicians Gary Davies and Luke Bedford, for their assistance in the experimental work. The research described in this paper has been co-financed by the UK Engineering and Physical Sciences Research Council (EP/L50502X/1) and the University of Nottingham through the Dean of Engineering Prize, a scheme for pump priming support for early career academic staff.

## References

- [1] Triantafillou TC. Shear strengthening of reinforced concrete beams using epoxy-bonded FRP composites. *ACI Struct J* 1998;95(2):107–15.
- [2] Khalifa A, Gold WJ, Nanni A, MI AA. Contribution of externally bonded FRP to shear capacity of RC flexural members. *J Comp Constr* 1998;2(4):195–202.
- [3] Boussselham A, Chaallal O. Behavior of reinforced concrete T-beams strengthened in shear with carbon fiber-reinforced polymer—an experimental study. *ACI Struct J* 2006;103(3):339.
- [4] Chen JF, Teng JG. Shear capacity of fiber-reinforced polymer-strengthened reinforced concrete beams: fiber reinforced polymer rupture. *J Struct Eng* 2003a;129(5):615–25.
- [5] Chen JF, Teng JG. Shear capacity of FRP-strengthened RC beams: FRP debonding. *Constr Build Mat* 2003b;17(1):27–41.
- [6] Galal K, Mofidi A. Shear strengthening of RC T-beams using mechanically anchored unbonded dry carbon fiber sheets. *J Perform Constr Facil* 2010;24(1):31–9.
- [7] Mofidi A, Thivierge S, Chaallal O, Shao Y. Behavior of reinforced concrete beams strengthened in shear using L-shaped CFRP plates: experimental investigation. *J Comp Constr* 2014;18(2):04013033. [http://dx.doi.org/10.1061/\(ASCE\)CC.1943-5614.0000398](http://dx.doi.org/10.1061/(ASCE)CC.1943-5614.0000398).
- [8] Koutas L, Triantafillou TC. Use of anchors in shear strengthening of reinforced concrete T-beams with FRP. *J Comp Constr* 2013;17(1):101–7.
- [9] El-Saikaly G, Godat A, Chaallal O. New anchorage technique for FRP shear-strengthened RC T-Beams using CFRP rope. *J Comp Constr* 2014. [http://dx.doi.org/10.1061/\(ASCE\)CC.1943-5614.0000530](http://dx.doi.org/10.1061/(ASCE)CC.1943-5614.0000530).
- [10] Triantafillou TC, Papanicolaou CG, Zissimopoulos P, Laourdekis T. Concrete confinement with textile-reinforced mortar jackets. *ACI Struct J* 2006;103(1):28–37.
- [11] Bournas DA, Triantafillou TC, Zygouris K, Stavropoulos F. Textile-reinforced mortar versus FRP jacketing in seismic retrofitting of RC columns with continuous or Lap-spliced deformed bars. *J Comp Constr* 2009;13(5):360–71.
- [12] Ortlepp R, Lorenz A, Curbach M. Column strengthening with TRC: influences of the column geometry onto the confinement effect. *Adv Mater Sci Eng* 2009;2009:5. Article ID 493097. <http://dx.doi.org/10.1155/2009/493097>.
- [13] Bournas DA, Triantafillou TC. Bond strength of lap-spliced bars in concrete confined with composite jackets. *J Comp Constr* 2011;15(2):156–67.
- [14] Bournas DA, Triantafillou TC. Bar buckling in RC columns confined with composite materials. *J Comp Constr* 2011;15(3):393–403.
- [15] Al-Salloum YA, Siddiqui NA, Elsanadedy HM, Abadel AA, Aqel MA. Textile-reinforced mortar versus FRP as strengthening material for seismically deficient RC beam-column joints. *J Comp Constr* 2011;15(6):920–33.
- [16] D'Ambrisi A, Feo L, Focacci F. Experimental analysis on bond between PBO-FRCM strengthening materials and concrete. *Compos Part B* 2013;44(1):524–32.
- [17] Elsanadedy HM, Almusallam TH, Alsayed SH, Al-Salloum YA. Flexural strengthening of RC beams using textile reinforced mortar—Experimental and numerical study. *J Comp Struct* 2013;97:40–5.
- [18] Bournas DA, Pavese A, Tizani W. Tensile capacity of FRP anchors in connecting FRP and TRM sheets to concrete. *Engin Struct* 2015;82(1):72–81.
- [19] D'Ambrisi A, Feo L, Focacci F. Bond-slip relations for PBO-FRCM materials externally bonded to concrete. *Compos Part B* 2012;43(8):2938–49.
- [20] Pellegrino C, D'Antino T. Experimental behaviour of existing precast prestressed reinforced concrete elements strengthened with cementitious composites. *Compos Part B* 2013;55:31–40.
- [21] Larrinaga P, Chastre C, San-José JT, Garmendia L. Non-linear analytical model of composites based on basalt textile reinforced mortar under uniaxial tension. *Compos Part B* 2013;55:518–27.
- [22] Koutas L, Bousias SN, Triantafillou TC. Seismic strengthening of masonry-infilled RC frames with TRM: experimental study. *J Comp Constr* 2015;19(2):04014048. [http://dx.doi.org/10.1061/\(ASCE\)CC.1943-5614.0000507](http://dx.doi.org/10.1061/(ASCE)CC.1943-5614.0000507).
- [23] Bousias S, Spathis AL, Fardis M, Triantafillou TC, Papanicolaou C. Pseudodynamic tests of non-seismically designed RC structures retrofitted with textile reinforced mortar. In: *Proc 8th Int Symp on fiber reinforced polymer reinforcement for concrete structures (FRPRCS-8)*, Patras, Greece; 2007.
- [24] ACI 549.4R-13. *Guide to Design and Construction of Externally Bonded Fabric-Reinforced Cementitious Matrix (FRCM) Systems for Repair and Strengthening Concrete and Masonry Structures*.
- [25] Triantafillou TC, Papanicolaou CG. Shear strengthening of reinforced concrete members with textile reinforced mortar (TRM) jackets. *Mater Struct* 2006;39(1):93–103.
- [26] Brückner A, Ortlepp R, Curbach M. Anchoring of shear strengthening for T-beams made of textile reinforced concrete (TRC). *Mater Struct* 2008;41(2):407–18.
- [27] Al-Salloum YA, Elsanadedy HM, Alsayed SH, Iqbal RA. Experimental and numerical study for the shear strengthening of reinforced concrete beams using textile-reinforced mortar. *J Comp Constr* 2012;16(1):74–90.
- [28] Azam R, Soudki K. FRCM strengthening of shear-critical RC beams. *J Comp Constr* 2014;18(5):04014012. [http://dx.doi.org/10.1061/\(ASCE\)CC.1943-5614.0000464](http://dx.doi.org/10.1061/(ASCE)CC.1943-5614.0000464).
- [29] Tzoura E, Triantafillou TC. Shear strengthening of reinforced concrete T-beams under cyclic loading with TRM or FRP jackets. *Mater Struct* 2014. <http://dx.doi.org/10.1617/s11527-014-0470-9>.
- [30] Pellegrino C, Vasic M. Assessment of design procedures for the use of externally bonded FRP composites in shear strengthening of reinforced concrete beams. *Compos Part B* 2013;45(1):727–41.
- [31] EN 1015-11. *Methods of test for mortar for masonry – Part 11: determination of flexural and compressive strength of hardened mortar*. Brussels: Comité Européen de Normalisation; 1993.
- [32] Triantafillou TC, Antonopoulos CP. Design of concrete flexural members strengthened in shear with FRP. *J Comp Constr* 2000;4(4):198–205.